Science Advances
AAAS

Supplementary Materials for

Mechanisms of antigen-induced reversal of CNS inflammation in experimental demyelinating disease

Jian Li *et al.*

Corresponding author: Michael J. Lenardo, lenardo@nih.gov; Lixin Zheng, lzheng@niaid.nih.gov; Yu-zhang Wu, wuyuzhang@tmmu.edu.cn; Zhihong Zhang, czyzzh@mail.hust.edu.cn

Sci. Adv. **9**, eabo2810 (2023)
DOI: 10.1126/sciadv.abo2810

The PDF file includes:

Other Supplementary Material for this manuscript includes the following:

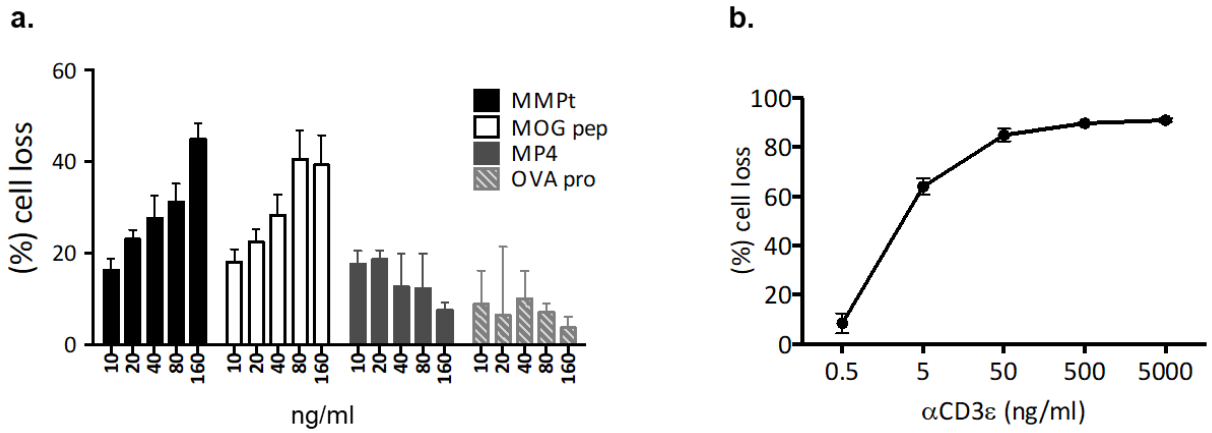

Fig. S1 MMPt therigen specifically induces RICD of MOG specific T cells *in vitro*. a. Percent loss of viable cell counts for the activated 2D2-TCR-tg (MOGp35~55 specific) and OT-II (OVAp323~339) T cells in response to stimulations of MMPt, MOGp35~55, MP4, and OVA protein at indicated doses for 48 hours in the presence of irradiated syngeneic splenocytes. **b.** Percent cell loss of activated 2D2 TCR-Tg T cells in response to *in vitro* anti-CD3e stimulation at the indicated doses for 48 hours. Data represent > 2 independent experiments.

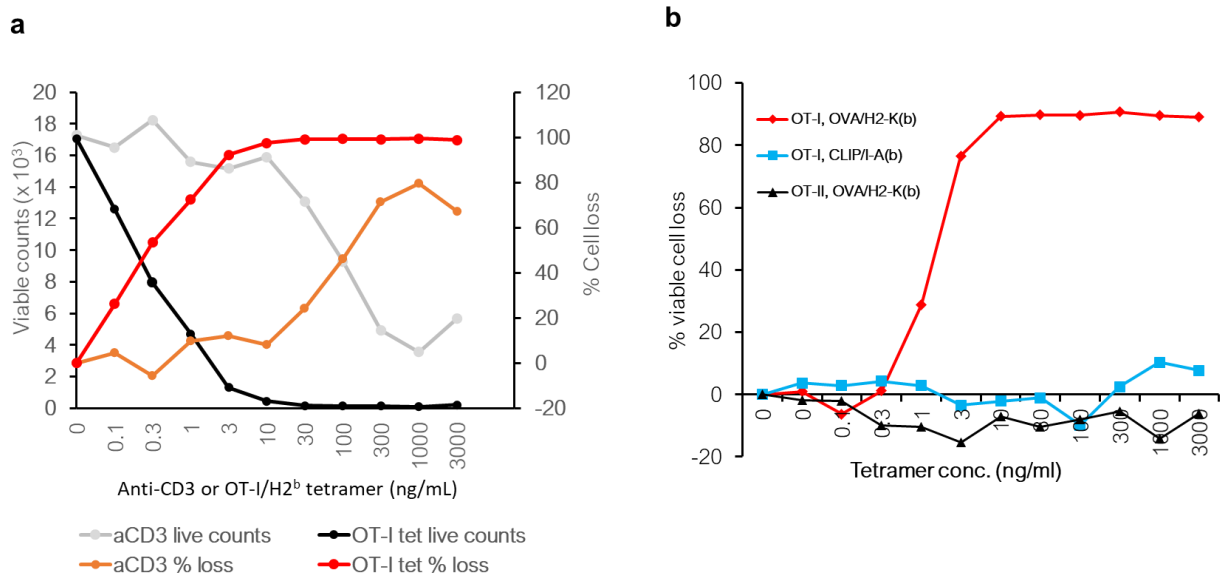

Fig. S2. Dose dependence and TCR specificity of activated mouse primary T cell RICD *in vitro*. Lymph node T cells from a C57BL/6 OT-I mouse was isolated and stimulated with 3 ug/mL concanavalin A for 2 days, and subsequently treated with 100 IU/mL IL2 complete RPMI media in culture for 6 days before subjected to the serial dilutions of mass matched amounts of anti-CD3 (2C11-145 with 2 x of protein A), or OT-I (SIIFENKL/H2K(b)) tetramer stimulation for 48 hours in culture. **a.** Viable cell counts (left Y axis) and percent of cell loss (right Y axis) data are plotted on doses of TCR stimulation as indicated in the x axis. **b.** Percent loss of activated OT-I or OT-II Tg T cells responses to the indicated doses of tetramer stimulations for 48 hours, red diamonds: OT-I T cells in response to OVAp/H2-K(b) tetramer, blue squares: OT-I T cells response to class-II tetramer control CLIP/I-A(b), black triangles: OT-II T cells in response over the OT-I specific OVAp/H2-K(b).

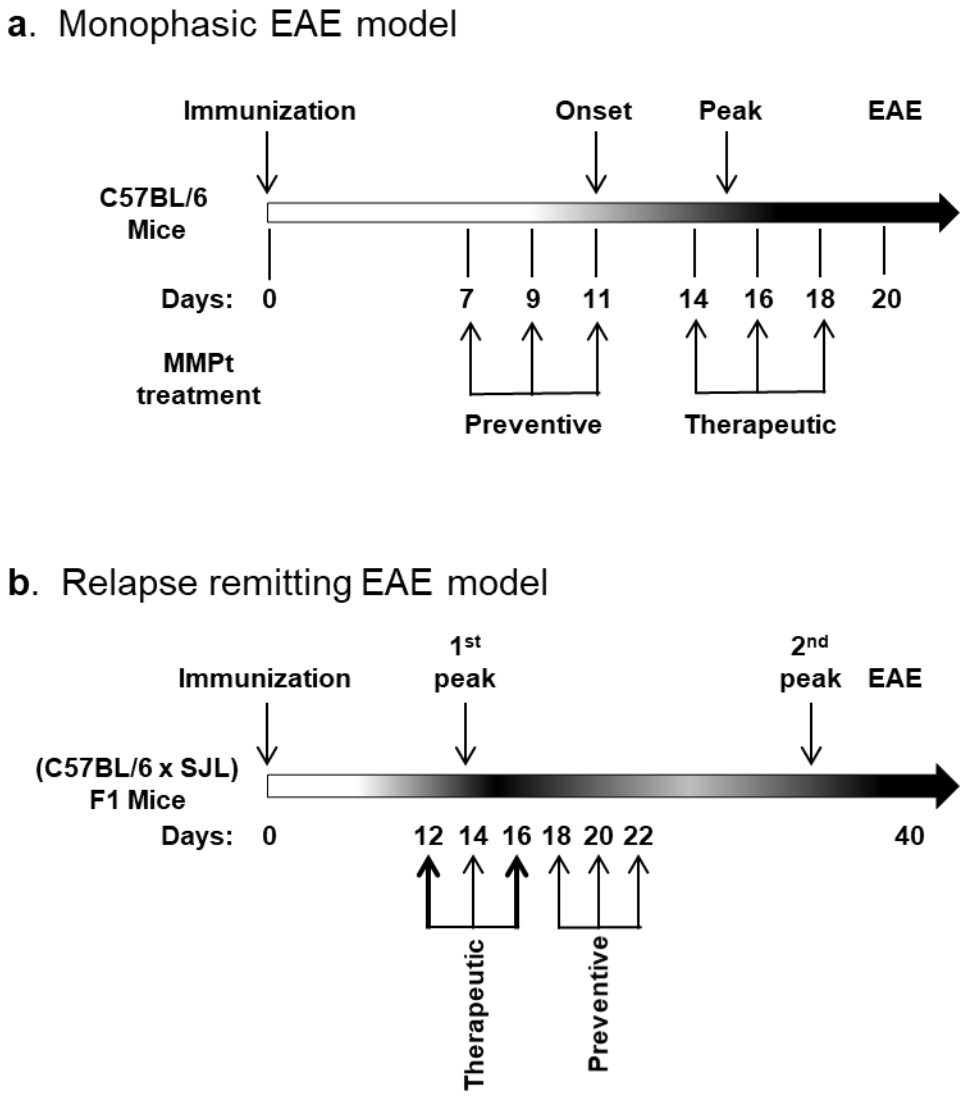

Fig. S3. MMPt treatment on MOGp35~55 (MOGp) induced monophasic and relapse-remitting (RR) EAE diseases in mice. a. Experimental design for therapeutic and preventive treatments of MOGp-induced monophasic mouse EAE. C57BL/6 mice immunized at day 0 are subjected to 400 ug per mouse IV injection twice daily at the indicated days after EAE induction. **b.** Schematic presentation of the therapeutic and relapse-preventive interventions over the timeline of the MOGp-induced RR EAE in C57BL/6 x SJL F1 mice. Gradient intensity reflects development and severity of EAE disease signs in both the monophasic and the RR EAE models.

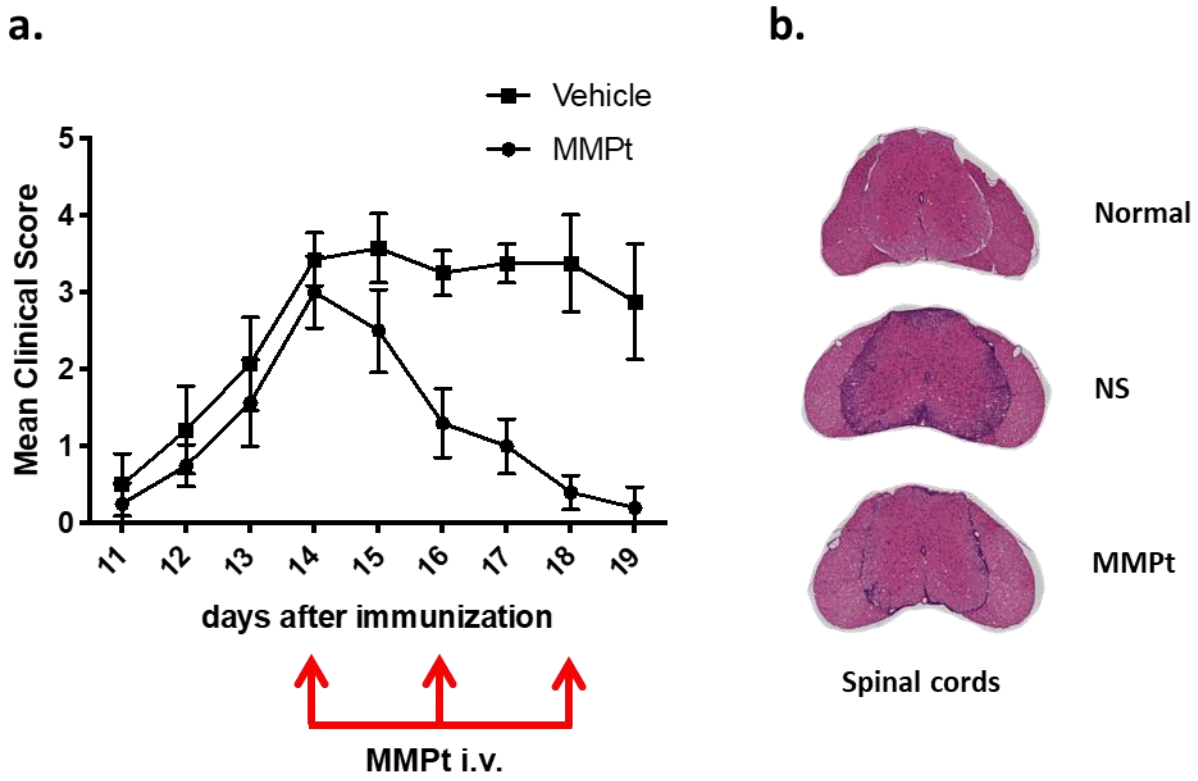

Fig. S4. **Therapeutical effect of MMPt on established EAE in C57BL/6 mice**. **a.** one representative experiment depicting the peak of MOGp-induced score 3+ EAE mice (n=5 each group) received 6 doses vehicle or MMPt at 0.4 mg i.v. twice per every other day as indicated in red arrows (day 14, 16, and 18 post EAE induction). **b.** Histopathological H&E staining of spinal cord sections representatively showing reduction of CNS inflammatory cell infiltration in EAE mice treated by the MMPt. Representative spinal cord sections from as indicated a normal mouse (upper), the day-20, 3-dose vehicle of normal saline (NS, middle) or 800 ug MMPt treated (bottom) in MOGp-induced EAE mice.

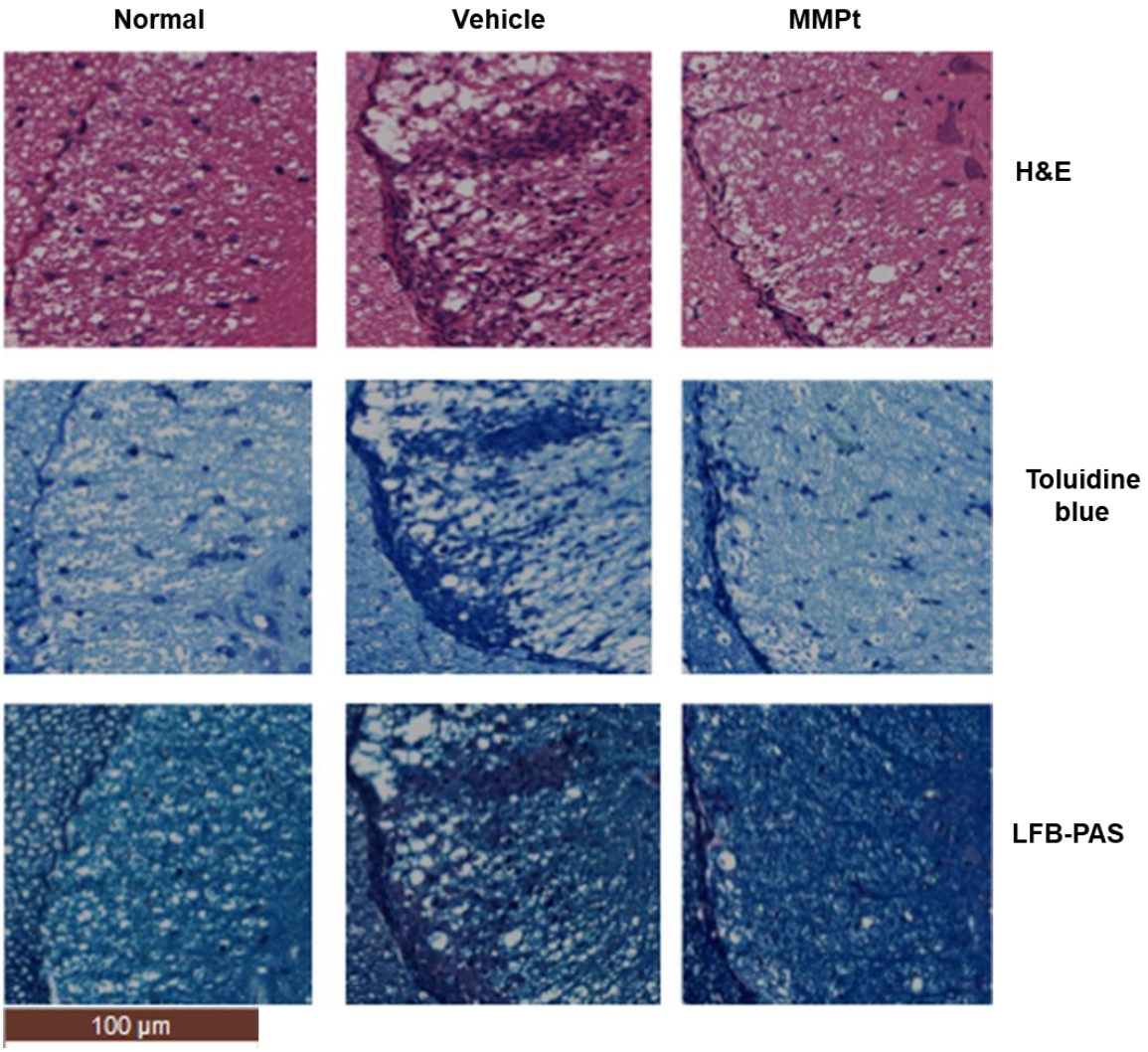

Fig. S5 MMPt treatment significantly improves pathological myelin damage in the spinal cord of MOGp-induced C57BL/6 EAE mice. Histopathological analysis of lumbar spinal cord sections from mice of normal (left panels), day 20 post induction of EAE treated with normal saline vehicle (middle panels), and day-20 EAE animal treated with 3 doses of MMPt as depicted in Suppl. Fig. S2a. Sections were stained by H&E (upper), Myelin stain by toluidine blue (middle), and another myelin staining dye Luxol fast blue-Periodic acid Schiff (LFB-PAS, bottom panel).

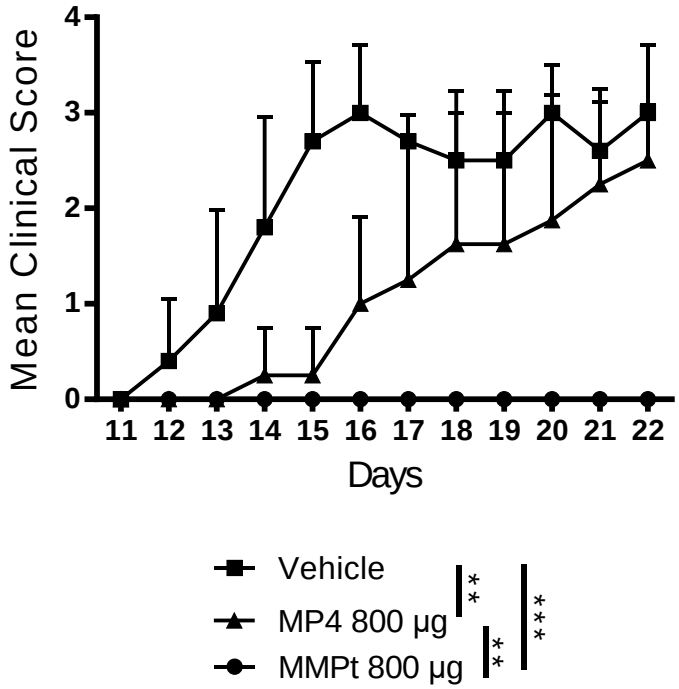

Fig. S6. MMPt show improved protection over MP4 on MOGp-induced EAE in C57BL/6 mice. Mice were immunized for EAE induction on day 0 by using MOGp35~55 Hook's Lab kit. Data display the EAE clinical scores of the EAE-induced mice that were subjected to i.v. injections at day 8, 10, and 12 with vehicle (n=5), or 800 ug of MMPt (n=5), or 800 ug of MP4 (n=5) as indicated. Statistical analysis was performed using Student's t-test and two-way annova with Tukey's multiple comparison, ** $p < 0.01$, *** $p < 0.001$. Data represents 1 of 2 independent experiments.

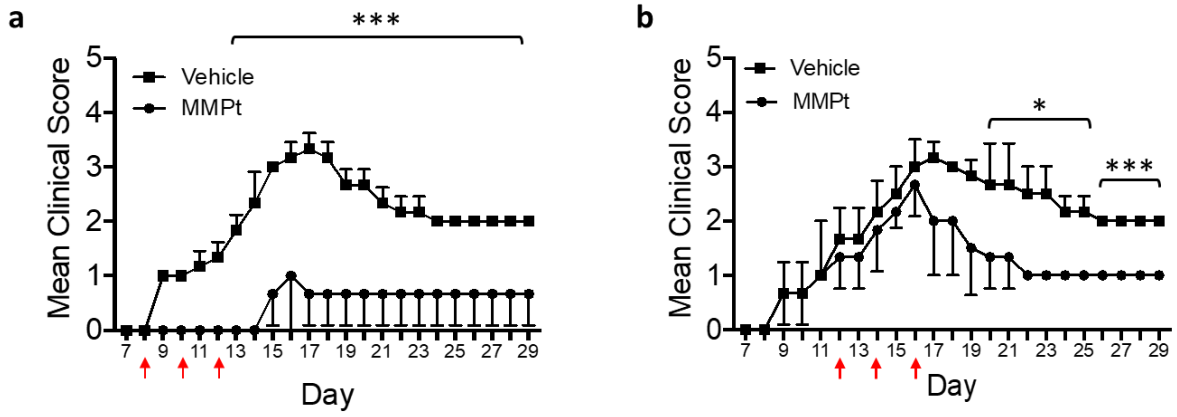

Fig. S7. MMPt show therapeutic and preventive effect on mouse spinal-cord (SC) homogenate-induced EAE in C57BL/6 mice. Mice were injected subcutaneously with spinal cord homogenate emulsion, 100 uL (~ 4 mg spinal cord mass) in each of the upper and lower back locations on day 0, along with 400 ng pertussis toxin intraperitoneally injections at 2 hours and 24 hours per mouse after the SC homogenate. **a.** EAE mean clinical scores of mice that were treated at day 8, 10, and 12 with vehicle (squares, n=3), or 200 ug MMPt (circles, n=3) via i.v. injections (red arrows). **b.** EAE mean clinical scores of mice after disease establishment that were treated at day 12, 14, and 16 with vehicle (squares, n=3), or 200 ug MMPt (circles, n=3) via i.v. injections as indicated by the red arrows. One-way ANOVA with Tukey's multiple comparisons was used for statistical tests, * $p < 0.05$, *** $p < 0.001$, **** $p < 0.0001$.

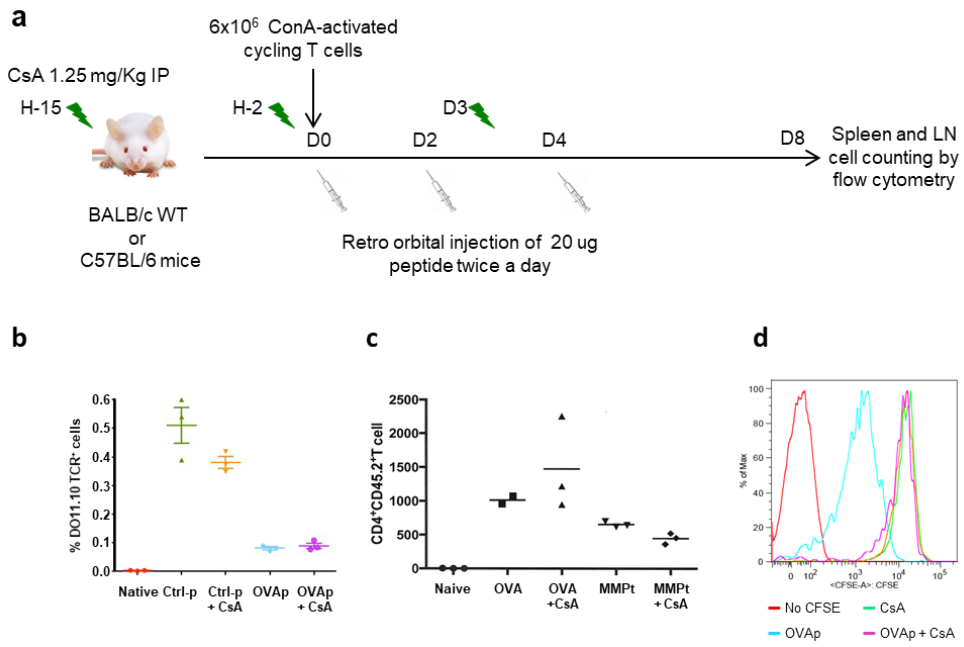

Fig. S8. **RICD is antigen specific and resistant to cyclosporin inhibition**.

a, the sketch of in vivo RICD experiment by adoptive transfer of activated DO11.10, OVA323-339 peptide(OVAp)-specific TCR transgenic T cells into BALB/c mice, or MOGp35-55 specific 2D2 TCR-Tg T cells into C57BL/6 mice, treated with and without cyclosporin A (CsA) as indicated, and subsequently encountering the mice with repeated OVA peptide stimulations as indicated in the time course for induction of RICD. **b,** loss of the adoptively transferred OVAp-specific T cells in the spleens and lymph nodes of recipient mice. Percent of adopted T cells under indicated experimental conditions are shown. After 2 injections of 1.25 mg/kg CsA via IP at hour -15 and hour -2, 6-million pre-activated DO11.10 T cells (in vitro pre activation with 1 ug/mL concanavalin A (Con A) for 3 days and cycling for 2 days in culture with 100U/mL of IL-2) were injected by IV in 8~12-week-old BALB/c female mice (n=3 per group). Mice were treated on D0, D2, D4 twice daily with IV injections of 20 ug control (scrambled peptides) or OVA323-339 peptides. A third injection of CsA was given on D3 (1.25 mg/Kg, IP). On day 4, splenocytes and LN cells were analyzed by flow cytometry. **c,** MMPt specifically deplete MOGp-reactive T cells in a CsA resistant manner *in vivo*. CD45.1 C57/BL mice (8 ~ 12-wk-old, n=3) were injected via IP with 1.25 mg/Kg CsA at 15 hours and 2 hours before adoptive IV transfer of $6x10^6$ of pre-activated 2D2 T cells (*same as in panel **a***). Mice were subjected on D0, D2, with IV 400ug twice/day of MMPt or OVA protein. On D8, splenocytes and LN cells were quantified by flow cytometry, n=3 for each group. **d,** Flowcytometry CFSE assay showing in *vitro* inhibition of activation and proliferation of DO11.10 TCR-Tg T cells in response to OVAp stimulation in the presence of absence of 1 ug/ mL CsA for 5 days. DO11.10 TCR-Tg T cells were isolated and labeled with CFSE before subjected to 10 uM of OVA323~339 peptide loaded on irradiated syngeneic mouse splenocytes for 3 days and subsequently treated with 100 IU/mL IL2 in culture for 2 days. Samples in the CFSE histograms are as indicated in corresponding to the day-5 cell cultures.

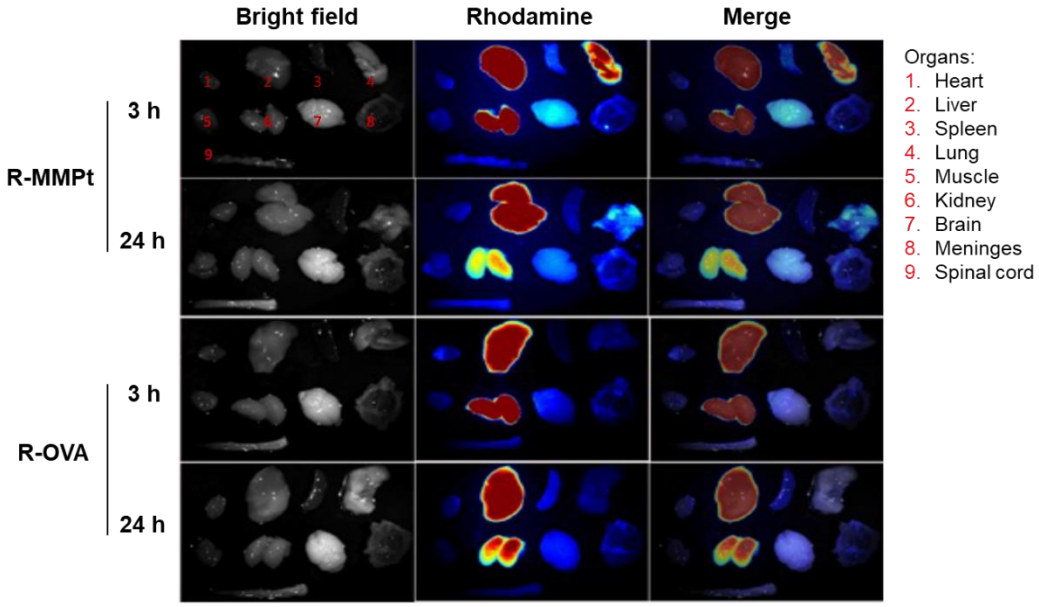

Fig. S9. Tissue distribution of therigen protein through intravenous injection in MOG-induced C57BL/6 EAE mice. *Ex vivo* fluorescence imaging of organs removed from EAE mice with a clinical score of 3 that were sacrificed 3 hours or 24 hours after tail vein injection of rhodamine-conjugated MMPt (R-MMPt) or rhodamine conjugated ovalbumin (R-OVA). Bright field (left panels), fluorescence images (middle panels), merged images (right panels). Organs are annotated in order as shown in the upper left image.

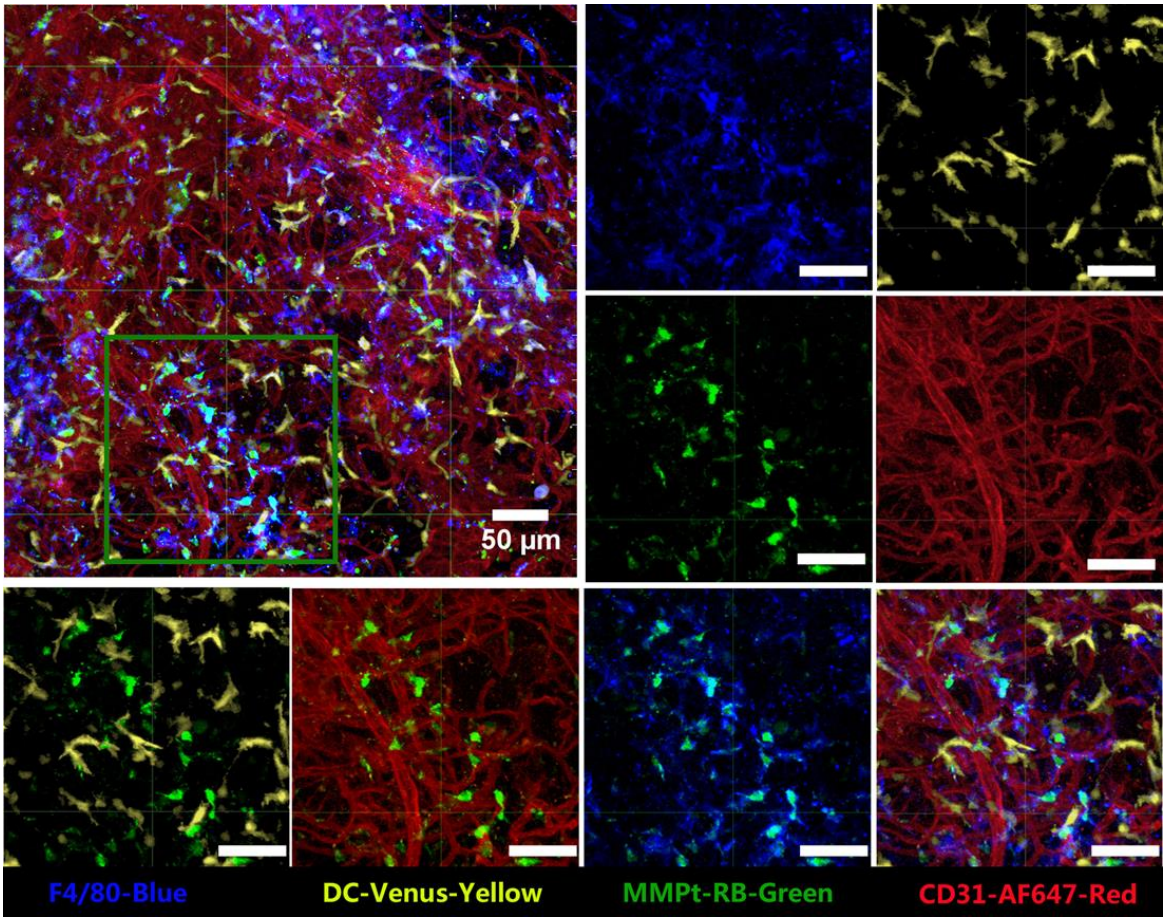

Fig. S10. Uptake of therigen MMPt by perivascular macrophages but not DCs in the CNS of MOGp-induced C57BL/6 EAE mice. Confocal microscopy imaging of the EAE spinal cord section at 1 hour after MMPt IV injection. The examined cell populations are shown in individually assigned wavelength channels and the corresponding merged images, F4/80 for macrophages (blue), DC-Venus for DC (yellow), CD31 for blood vessel endothelia (red), and MMPt (green). All scale bars equal 50 µm.

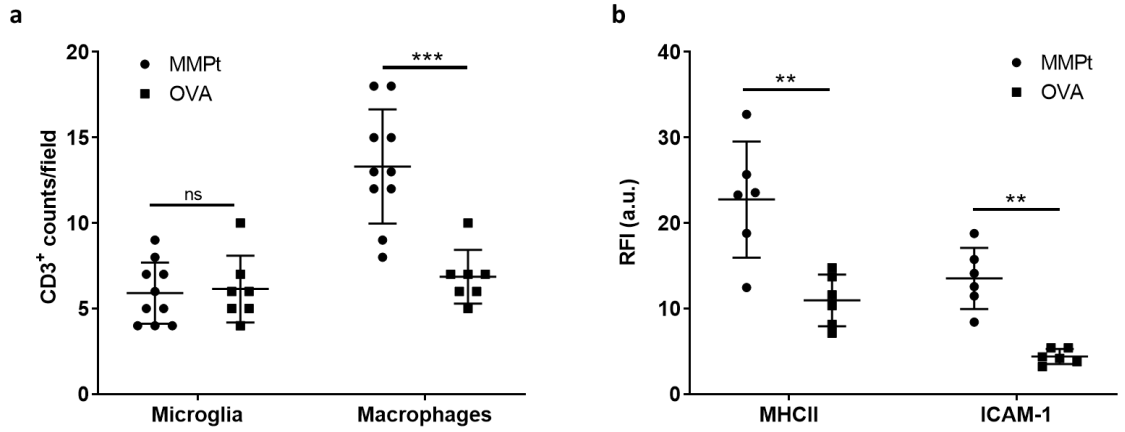

Fig S11. MMPt induces interactions of infiltrating T cells with local macrophages in the CNS of EAE mice. a, The number of $CD3^+$ T cells per field in contact with microglia (10 fields) or macrophages (7 fields) of images taken from IVM images of the spinal cords of EAE mice that were injected IV with MMPt or Ova proteins for 1 hour as indicated in Fig 2. **b**, Relative fluorescence intensities (RFI) per field (n=6) of essential components of the immune synapse MHCII and ICAM-1 are shown for immunofluorescent staining of the spinal cord sections of EAE mice treated with MMPt or OVA proteins as indicated in Fig 3. Data analyses were automatically generated by Image J software. The unpaired t-test was used for statistics, ** $p < 0.01$, *** $p < 0.001$. Data represent two independent experiments.

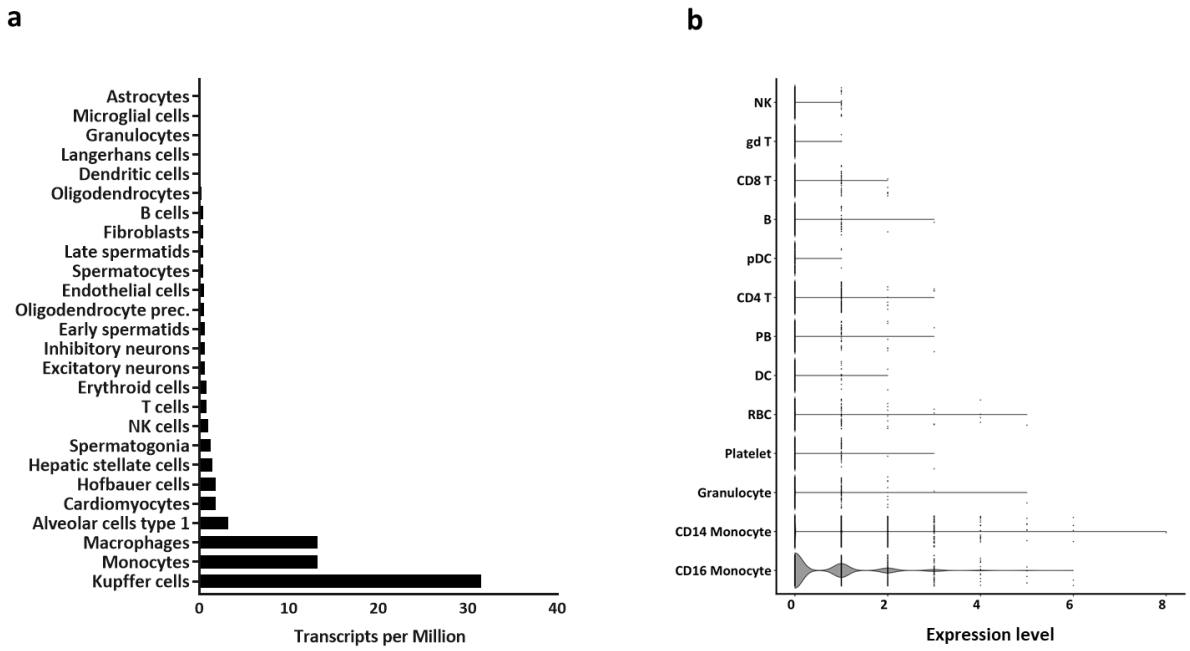

Fig. S12 Human monocytes/macrophages express ADGRE1/EMR1. a. Analysis of single cell RNAseq data (Human Protein Atlas, https://www.proteinatlas.org/) shows tissue-specific expression of normalized transcripts per million (NTM) ADGRE1/EMR1 mRNA in selected types of cells in humans. **b.** A violin plot displays co-expression of ADGRE1/EMR1 genes with CD16 mainly in a subset of monocytes but not in other human blood cell types, including $CD14^{+}$ monocytes. The annotated data set is analyzed with Seurat (v.4.1.0) in Rstudio (v.1.3.1056). Shown are single cell ADGRE1/EMR1 expression levels per indicated cell types, from analysis of a publicly available data set (81).

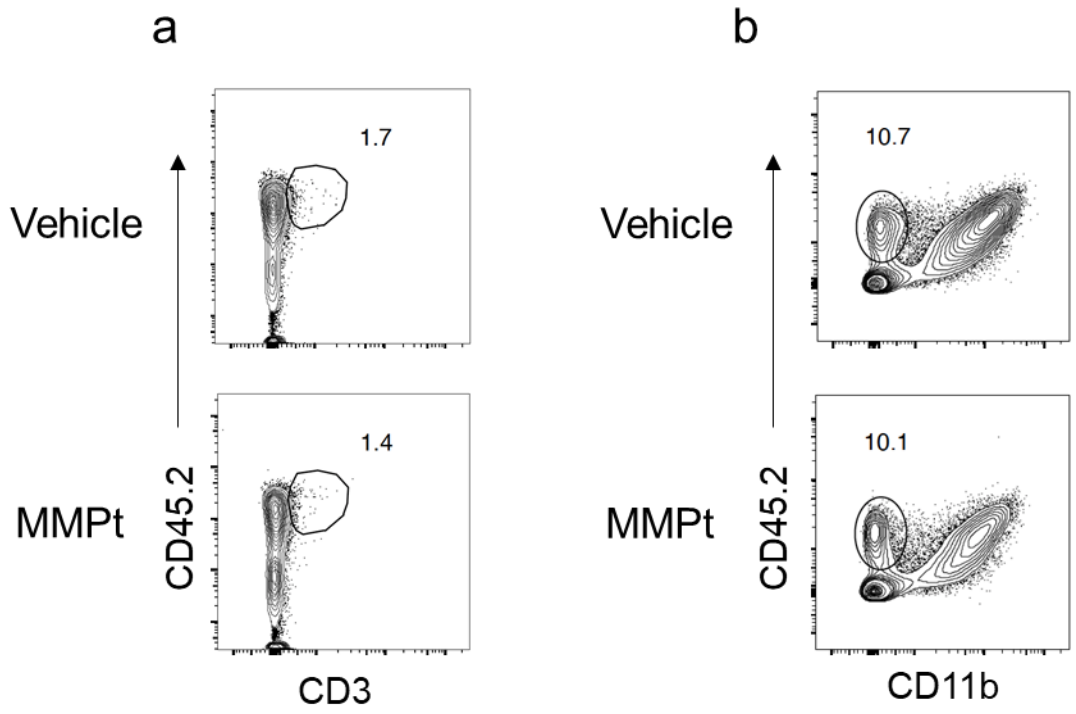

Fig. S13. Gating strategy for T cells from the isolated spinal cord mononuclear cells. a, gating on $CD3^+$, $CD45.2^+$ T cells for Figure 6 a ~ c**;** and **b**, gating on $CD11b^-$, $CD45.2^+$ T cells for Figure 6d.

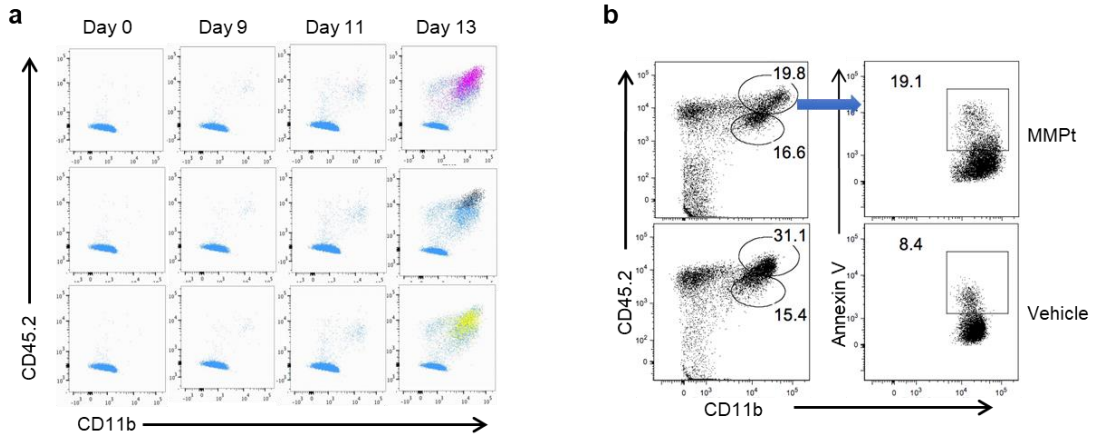

Fig. S14. **MMPt treatment on MOGp35~55 induced EAE in C57BL/6 mice associate with significant apoptosis of monocytes in the affected spinal cord tissue. a.** Flowcytometry staining CD11b and CD45.2 on monocytes isolated from the spinal cords at day 0, 9, 11, and 13 of the MOGp35~55 EAE induction, showing dynamics of spinal cord infiltrating leukocytes and activated local microglia during EAE induction in mice. Upper panels: total spinal cord leukocytes ($CD11b^{+}CD45^{+}$ in purple); Middle panels: the spinal cord infiltrating monocytes ($CD11b^{+}CD45^{high}$ in black; Bottom panels: activated microglia ($CD11b^{+}CD45^{int}$ in yellow). **b.** Flowcytometry showing annexin V positive apoptotic $CD11b^{+}CD45^{high}$ monocytes in the spinal cord of EAE mice on day 15 of EAE induction (24 hours after the first dose of MMPt/Vehicle treatment) in reference to the experimental schedule shown in figure S2a. Data represent 2 independent experiments for panel b.

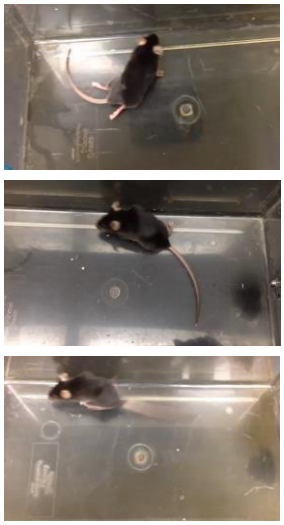

Movie S1

Movie S1. Therigen presentation to endogenous T cells in the CNS of MOGp-induced C57BL/6 EAE mice. Intravital two-photon microscopy movies showing rhodamine-conjugated MMPt (R-MMPt, red) presentation to the EAE infiltrating T cells (CXCR6-GFP, green) in the spinal cord of a score-3 established EAE mouse. Video clips were recorded for 5 minutes at 1 hour post R-MMPt injection (left), and 7minutes 50 seconds at 4 hours post the injection of R-MMPt. The endogenous CNS infiltrating green T cells migrate to macrophages and forming immune synapses as visualized by the marked circles, which is in contrast to DCs (Venus yellow) that did not show measurable interactions with T cells as shown in Suppl. Fig. S7.

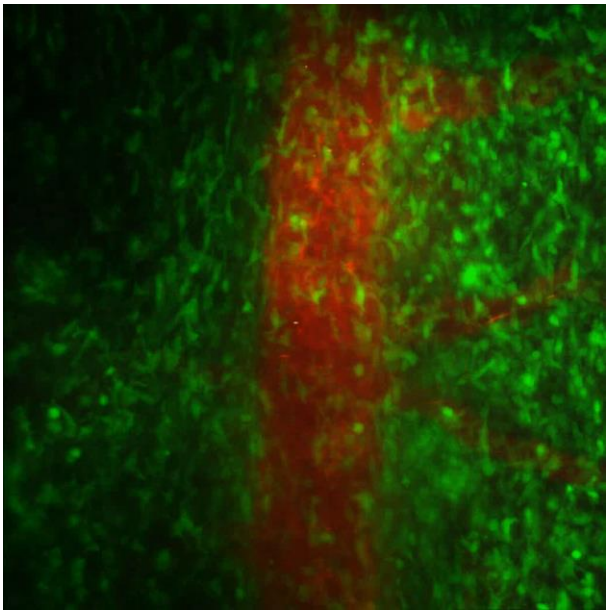

Movie S2. Meningeal antigen-presenting cells quickly capture therigen protein. Intravital two-photon microscopy movie clip showing kinetic distribution of the therigen MMPt from a blood vessel in the spinal cord meningeal area of a CX3CR1-GFP (microglia specific) transgenic EAE mouse in real time. The movie recording started within a few seconds after the IV injection of rhodamine-conjugated MMPt (R-MMPt), and lasted for 30 minutes, with R-MMPt in red and microglia in green. Data represent two independent experiments.

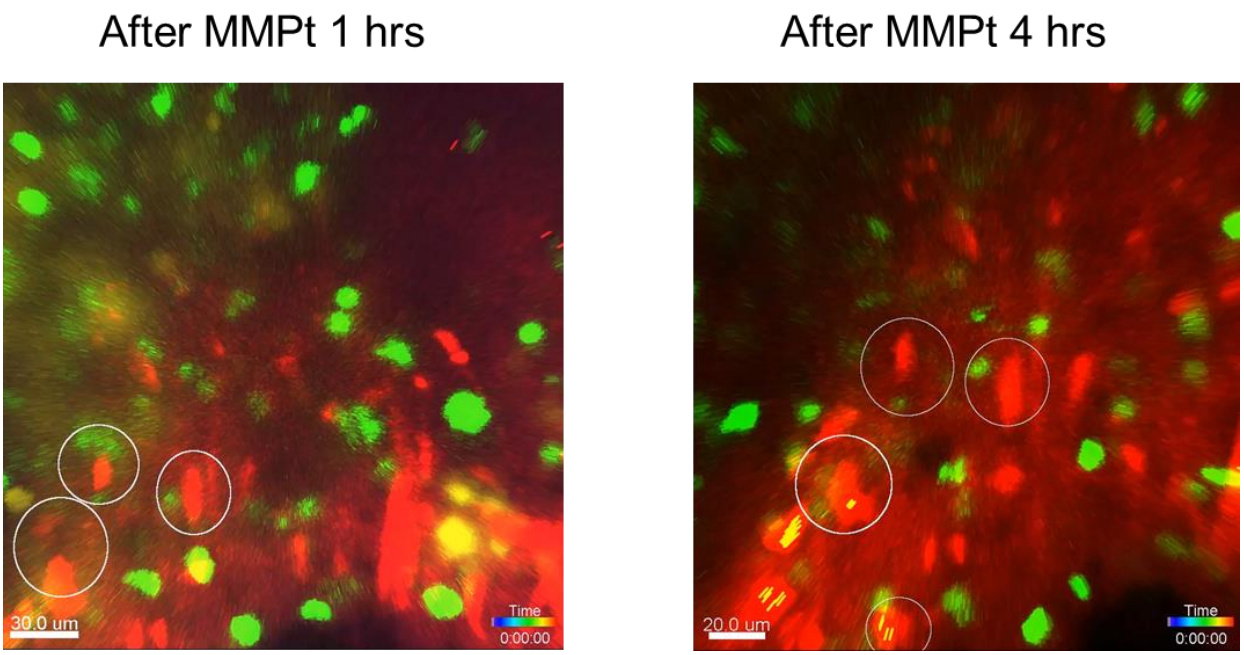

Movie S3. Therigen presentation to endogenous T cells in the CNS of MOGp-induced C57BL/6 EAE mice. Intravital two-photon microscopy movies showing rhodamine-conjugated MMPt (R-MMPt, red) presentation to the EAE infiltrating T cells (CXCR6-GFP, green) in the spinal cord of a score-3 established EAE mouse. Video clips were recorded for 5 minutes at 1 hour post R-MMPt injection (left), and 7minutes 50 seconds at 4 hours post the injection of R-MMPt. The endogenous CNS infiltrating green T cells migrate to macrophages and forming immune synapses as visualized by the marked circles, which contrasts with DCs (Venus yellow) that did not show measurable interactions with T cells as shown in Suppl. Fig. S7.

REFERENCES AND NOTES

1. D. S. Reich, C. F. Lucchinetti, P. A. Calabresi, Multiple sclerosis. *N. Engl. J. Med.* **378**, 169–180 (2018).

2. Global, regional, and national burden of neurological disorders during 1990-2015: A systematic analysis for the Global Burden of Disease Study 2015. *Lancet Neurol.* **16**, 877–897 (2017).

3. H. E. Titus, Y. Chen, J. R. Podojil, A. P. Robinson, R. Balabanov, B. Popko, S. D. Miller, Pre-clinical and clinical implications of "Inside-Out" vs. "Outside-In" paradigms in multiple sclerosis etiopathogenesis. *Front. Cell. Neurosci.* **14**, 599717 (2020).

4. M. Naegele, R. Martin, The good and the bad of neuroinflammation in multiple sclerosis. *Handb. Clin. Neurol.* **122**, 59–87 (2014).

5. E. Bettelli, M. P. Das, E. D. Howard, H. L. Weiner, R. A. Sobel, V. K. Kuchroo, IL-10 is critical in the regulation of autoimmune encephalomyelitis as demonstrated by studies of IL-10- and IL-4-deficient and transgenic mice. *J. Immunol.* **161**, 3299–3306 (1998).

6. R. C. Coll, A. A. B. Robertson, J. J. Chae, S. C. Higgins, R. Muñoz-Planillo, M. C. Inserra, I. Vetter, L. S. Dungan, B. G. Monks, A. Stutz, D. E. Croker, M. S. Butler, M. Haneklaus, C. E. Sutton, G. Núñez, E. Latz, D. L. Kastner, K. H. G. Mills, S. L. Masters, K. Schroder, M. A. Cooper, L. A. J. O'Neill, A small-molecule inhibitor of the NLRP3 inflammasome for the treatment of inflammatory diseases. *Nat. Med.* **21**, 248–255 (2015).

7. J. M. Frischer, S. Bramow, A. Dal-Bianco, C. F. Lucchinetti, H. Rauschka, M. Schmidbauer, H. Laursen, P. S. Sorensen, H. Lassmann, The relation between inflammation and neurodegeneration in multiple sclerosis brains. *Brain* **132**, 1175–1189 (2009).

8. L. Steinman, Immunology of relapse and remission in multiple sclerosis. *Annu. Rev. Immunol.* **32**, 257–281 (2014).

9. A. Ben-Nun, H. Wekerle, I. R. Cohen, The rapid isolation of clonable antigen-specific T lymphocyte lines capable of mediating autoimmune encephalomyelitis. *Eur. J. Immunol.* **11**, 195–199 (1981).

10. R. Martin, H. F. McFarland, Immunological aspects of experimental allergic encephalomyelitis and multiple sclerosis. *Crit. Rev. Clin. Lab. Sci.* **32**, 121–182 (1995).

11. F. Mokhtarian, D. E. McFarlin, C. S. Raine, Adoptive transfer of myelin basic protein-sensitized T cells produces chronic relapsing demyelinating disease in mice. *Nature* **309**, 356–358 (1984).

12. D. Ontaneda, A. J. Thompson, R. J. Fox, J. A. Cohen, Progressive multiple sclerosis: Prospects for disease therapy, repair, and restoration of function. *Lancet* **389**, 1357–1366 (2017).

13. J. Sellner, P. S. Rommer, A review of the evidence for a natalizumab exit strategy for patients with multiple sclerosis. *Autoimmun. Rev.* **18**, 255–261 (2019).

14. C. H. Polman, P. W. O'Connor, E. Havrdova, M. Hutchinson, L. Kappos, D. H. Miller, J. T. Phillips, F. D. Lublin, G. Giovannoni, A. Wajgt, M. Toal, F. Lynn, M. A. Panzara, A. W. Sandrock; AFFIRM Investigators, A randomized, placebo-controlled trial of natalizumab for relapsing multiple sclerosis. *N. Engl. J. Med.* **354**, 899–910 (2006).

15. J. R. Berger, Classifying PML risk with disease modifying therapies. *Mult. Scler. Relat. Disord.* **12**, 59–63 (2017).

16. A. Compston, A. Coles, Multiple sclerosis. *Lancet* **372**, 1502–1517 (2008).

17. M. Gasim, C. N. Bernstein, L. A. Graff, S. B. Patten, R. El-Gabalawy, J. Sareen, J. M. Bolton, J. J. Marriott, J. D. Fisk, R. A. Marrie; CIHR team "Defining the burden and managing the effects of psychiatric comorbidity in chronic inflammatory disease", Adverse psychiatric effects of disease-modifying therapies in multiple sclerosis: A systematic review. *Mult. Scler. Relat. Disord.* **26**, 124–156 (2018).

18. A. J. Coles, D. A. S. Compston, K. W. Selmaj, S. L. Lake, S. Moran, D. H. Margolin, K. Norris, P. K. Tandon, Alemtuzumab vs. interferon β-1a in early multiple sclerosis. *N. Engl. J. Med.* **359**, 1786–1801 (2008).

19. G. Mancardi, R. Saccardi, Autologous haematopoietic stem-cell transplantation in multiple sclerosis. *Lancet Neurol.* **7**, 626–636 (2008).

20. L. Steinman, P. P. Ho, W. H. Robinson, P. J. Utz, P. Villoslada, Antigen-specific tolerance to self-antigens in protein replacement therapy, gene therapy and autoimmunity. *Curr. Opin. Immunol.* **61**, 46–53 (2019).

21. M. J. Lenardo, lnterleukin-2 programs mouse αβ T lymphocytes for apoptosis. *Nature* **353**, 858–861 (1991).

22. L. Zheng, J. Li, M. Lenardo, Restimulation-induced cell death: New medical and research perspectives. *Immunol. Rev.* **277**, 44–60 (2017).

23. J. M. Critchfield, M. J. Lenardo, Antigen-induced programmed T cell death as a new approach to immune therapy. *Clin. Immunol. Immunopathol.* **75**, 13–19 (1995).

24. A. L. Snow, P. Pandiyan, L. Zheng, S. M. Krummey, M. J. Lenardo, The power and the promise of restimulation-induced cell death in human immune diseases. *Immunol. Rev.* **236**, 68–82 (2010).

25. G. Casella, J. Rasouli, A. Boehm, W. Zhang, D. Xiao, L. L. W. Ishikawa, R. Thome, X. Li, D. Hwang, P. Porazzi, S. Molugu, H. Y. Tang, G. X. Zhang, B. Ciric, A. Rostami, Oligodendrocyte-derived extracellular vesicles as antigen-specific therapy for autoimmune neuroinflammation in mice. *Sci. Transl. Med.* **12**, eaba0599 (2020).

26. G. D. Keeler, S. Kumar, B. Palaschak, E. L. Silverberg, D. M. Markusic, N. T. Jones, B. E. Hoffman, Gene therapy-induced antigen-specific tregs inhibit neuro-inflammation and reverse disease in a mouse model of multiple sclerosis. *Mol. Ther.* **26**, 173–183 (2018).

27. A. Lutterotti, H. Hayward-Koennecke, M. Sospedra, R. Martin, Antigen-specific immune tolerance in multiple sclerosis—Promising approaches and how to bring them to patients. *Front. Immunol.* **12**, 640935 (2021).

28. C. R. Gabaglia, A. T. Booker, T. A. Braciak, The potential for immunospecific therapy in multiple sclerosis based on identification of driver clones of the disease. *Crit. Rev. Immunol.* **40**, 237–246 (2020).

29. N. Kerlero de Rosbo, R. Milo, M. B. Lees, D. Burger, C. C. Bernard, A. Ben-Nun, Reactivity to myelin antigens in multiple sclerosis. Peripheral blood lymphocytes respond predominantly to myelin oligodendrocyte glycoprotein. *J. Clin. Invest.* **92**, 2602–2608 (1993).

30. M. Varrin-Doyer, A. Shetty, C. M. Spencer, U. Schulze-Topphoff, M. S. Weber, C. C. A. Bernard, T. Forsthuber, B. A. C. Cree, A. J. Slavin, S. S. Zamvil, MOG transmembrane and cytoplasmic domains contain highly stimulatory T-cell epitopes in MS. *Neurol. Neuroimmunol. Neuroinflamm.* **1**, e20 (2014).

31. J. M. Critchfield, M. K. Racke, J. C. Zúñiga-Pflücker, B. Cannella, C. S. Raine, J. Goverman, M. J. Lenardo, T cell deletion in high antigen dose therapy of autoimmune encephalomyelitis. *Science* **263**, 1139–1143 (1994).

32. C. E. Tadokoro, G. Shakhar, S. Shen, Y. Ding, A. C. Lino, A. Maraver, J. J. Lafaille, M. L. Dustin, Regulatory T cells inhibit stable contacts between $CD4^+$ T cells and dendritic cells in vivo. *J. Exp. Med.* **203**, 505–511 (2006).

33. X. Huang, H. Wu, Q. Lu, The mechanisms and applications of T cell vaccination for autoimmune diseases: A comprehensive review. *Clin Rev Allergy Immunol* **47**, 219–233 (2014).

34. J. Derdelinckx, P. Cras, Z. N. Berneman, N. Cools, Antigen-specific treatment modalities in MS: The past, the present, and the future. *Front. Immunol.* **12**, 624685 (2021).

35. F. Odoardi, N. Kawakami, Z. Li, C. Cordiglieri, K. Streyl, M. Nosov, W. E. F. Klinkert, J. W. Ellwart, J. Bauer, H. Lassmann, H. Wekerle, A. Flügel, Instant effect of soluble antigen on effector T cells in peripheral immune organs during immunotherapy of autoimmune encephalomyelitis. *Proc. Natl. Acad. Sci. U.S.A.* **104**, 920–925 (2007).

36. F. Odoardi, N. Kawakami, W. E. F. Klinkert, H. Wekerle, A. Flügel, Blood-borne soluble protein antigen intensifies T cell activation in autoimmune CNS lesions and exacerbates clinical disease. *Proc. Natl. Acad. Sci. U.S.A.* **104**, 18625–18630 (2007).

37. B. L. McRae, C. L. Vanderlugt, M. C. Dal Canto, S. D. Miller, Functional evidence for epitope spreading in the relapsing pathology of experimental autoimmune encephalomyelitis. *J. Exp. Med.* **182**, 75–85 (1995).

38. M. Yu, J. M. Johnson, V. K. Tuohy, A predictable sequential determinant spreading cascade invariably accompanies progression of experimental autoimmune encephalomyelitis: A basis for peptide-specific therapy after onset of clinical disease. *J. Exp. Med.* **183**, 1777–1788 (1996).

39. E. J. McMahon, S. L. Bailey, C. V. Castenada, H. Waldner, S. D. Miller, Epitope spreading initiates in the CNS in two mouse models of multiple sclerosis. *Nat. Med.* **11**, 335–339 (2005).

40. M. Lenardo, K. M. Chan, F. Hornung, H. McFarland, R. Siegel, J. Wang, L. Zheng, Mature T lymphocyte apoptosis–Immune regulation in a dynamic and unpredictable antigenic environment. *Annu. Rev. Immunol.* **17**, 221–53 (1999).

41. E. A. Elliott, H. I. McFarland, S. H. Nye, R. Cofiell, T. M. Wilson, J. A. Wilkins, S. P. Squinto, L. A. Matis, J. P. Mueller, Treatment of experimental encephalomyelitis with a novel chimeric fusion protein of myelin basic protein and proteolipid protein. *J. Clin. Invest.* **98**, 1602–1612 (1996).

42. S. D. Miller, D. M. Turley, J. R. Podojil, Antigen-specific tolerance strategies for the prevention and treatment of autoimmune disease. *Nat. Rev. Immunol.* **7**, 665–677 (2007).

43. D. P. McCarthy, M. H. Richards, S. D. Miller, Mouse models of multiple sclerosis: Experimental autoimmune encephalomyelitis and Theiler's virus-induced demyelinating disease. *Methods Mol. Biol.* **900**, 381–401 (2012).

44. L. Zheng, C. L. Trageser, D. M. Willerford, M. J. Lenardo, T cell growth cytokines cause the superinduction of molecules mediating antigen-induced T lymphocyte death. *J. Immunol.* **160**, 763–769 (1998).

45. M. Greter, F. L. Heppner, M. P. Lemos, B. M. Odermatt, N. Goebels, T. Laufer, R. J. Noelle, B. Becher, Dendritic cells permit immune invasion of the CNS in an animal model of multiple sclerosis. *Nat. Med.* **11**, 328–334 (2005).

46. M. Prinz, H. Schmidt, A. Mildner, K.-P. Knobeloch, U.-K. Hanisch, J. Raasch, D. Merkler, C. Detje, I. Gutcher, J. Mages, R. Lang, R. Martin, R. Gold, B. Becher, W. Brück, U. Kalinke, Distinct and nonredundant in vivo functions of IFNAR on myeloid cells limit autoimmunity in the central nervous system. *Immunity* **28**, 675–686 (2008).

47. C. Schläger, H. Körner, M. Krueger, S. Vidoli, M. Haberl, D. Mielke, E. Brylla, T. Issekutz, C. Cabañas, P. J. Nelson, T. Ziemssen, V. Rohde, I. Bechmann, D. Lodygin, F. Odoardi, A. Flügel, Effector T-cell trafficking between the leptomeninges and the cerebrospinal fluid. *Nature* **530**, 349–353 (2016).

48. J. Loos, S. Schmaul, T. M. Noll, M. Paterka, M. Schillner, J. T. Löffel, F. Zipp, S. Bittner, Functional characteristics of Th1, Th17, and ex-Th17 cells in EAE revealed by intravital two-photon microscopy. *J. Neuroinflammation* **17**, 357 (2020).

49. B. Rossi, G. Constantin, Live imaging of immune responses in experimental models of multiple sclerosis. *Front. Immunol.* **7**, 506 (2016).

50. G. Rougon, S. Brasselet, F. Debarbieux, Advances in intravital non-linear optical imaging of the central nervous system in rodents. *Brain Plast.* **2**, 31–48 (2016).

51. S. Stoll, J. Delon, T. M. Brotz, R. N. Germain, Dynamic imaging of T cell-dendritic cell interactions in lymph nodes. *Science* **296**, 1873–1876 (2002).

52. G. Mandolesi, A. Gentile, A. Musella, D. Fresegna, F. De Vito, S. Bullitta, H. Sepman, G. A. Marfia, D. Centonze, Synaptopathy connects inflammation and neurodegeneration in multiple sclerosis. *Nat. Rev. Neurol.* **11**, 711–724 (2015).

53. Y. Cao, B. A. Goods, K. Raddassi, G. T. Nepom, W. W. Kwok, J. C. Love, D. A. Hafler, Functional inflammatory profiles distinguish myelin-reactive T cells from patients with multiple sclerosis. *Sci. Transl. Med.* **7**, 287ra74 (2015).

54. M. S. Weber, T. Prod'homme, S. Youssef, S. E. Dunn, C. D. Rundle, L. Lee, J. C. Patarroyo, O. Stüve, R. A. Sobel, L. Steinman, S. S. Zamvil, Type II monocytes modulate T cell–mediated central nervous system autoimmune disease. *Nat. Med.* **13**, 935–943 (2007).

55. C. L. Mack, C. L. Vanderlugt-Castaneda, K. L. Neville, S. D. Miller, Microglia are activated to become competent antigen presenting and effector cells in the inflammatory environment of the Theiler's virus model of multiple sclerosis. *J. Neuroimmunol.* **144**, 68–79 (2003).

56. M. J. C. Jordão, R. Sankowski, S. M. Brendecke, Sagar, G. Locatelli, Y.-H. Tai, T. L. Tay, E. Schramm, S. Armbruster, N. Hagemeyer, O. Groß, D. Mai, Ö. Çiçek, T. Falk, M. Kerschensteiner, D. Grün, M. Prinz, Single-cell profiling identifies myeloid cell subsets with distinct fates during neuroinflammation. *Science* **363**, eaat7554 (2019).

57. I. Huitinga, N. van Rooijen, C. J. de Groot, B. M. Uitdehaag, C. D. Dijkstra, Suppression of experimental allergic encephalomyelitis in Lewis rats after elimination of macrophages. *J. Exp. Med.* **172**, 1025–1033 (1990).

58. M. M. Polfliet, P. H. Goede, E. M. van Kesteren-Hendrikx, N. van Rooijen, C. D. Dijkstra, T. K. van den Berg, A method for the selective depletion of perivascular and meningeal macrophages in the central nervous system. *J. Neuroimmunol.* **116**, 188–95 (2001).

59. M. M. Polfliet, F. van de Veerdonk, E. A. Döpp, E. M. van Kesteren-Hendrikx, N. van Rooijen, C. D. Dijkstra, T. K. van den Berg, The role of perivascular and meningeal macrophages in experimental allergic encephalomyelitis. *J. Neuroimmunol.* **122**, 1–8 (2002).

60. L. Ostendorf, P. Dittert, R. Biesen, A. Duchow, V. Stiglbauer, K. Ruprecht, J. Bellmann-Strobl, D. Seelow, W. Stenzel, R. A. Niesner, A. E. Hauser, F. Paul, H. Radbruch, SIGLEC1 (CD169): A marker of active neuroinflammation in the brain but not in the blood of multiple sclerosis patients. *Sci. Rep.* **11**, 10299 (2021).

61. A. Cugurra, T. Mamuladze, J. Rustenhoven, T. Dykstra, G. Beroshvili, Z. J. Greenberg, W. Baker, Z. Papadopoulos, A. Drieu, S. Blackburn, M. Kanamori, S. Brioschi, J. Herz, L. G. Schuettpelz, M. Colonna, I. Smirnov, J. Kipnis, Skull and vertebral bone marrow are myeloid cell reservoirs for the meninges and CNS parenchyma. *Science* **373**, eabf7844 (2021).

62. A. Wlodarczyk, M. Løbner, O. Cédile, T. Owens, Comparison of microglia and infiltrating $CD11c^+$ cells as antigen presenting cells for T cell proliferation and cytokine response. *J. Neuroinflammation* **11**, 57 (2014).

63. S. Gordon, J. Hamann, H. H. Lin, M. Stacey, F4/80 and the related adhesion-GPCRs. *Eur. J. Immunol.* **41**, 2472–2476 (2011).

64. D. Mrdjen, A. Pavlovic, F. J. Hartmann, B. Schreiner, S. G. Utz, B. P. Leung, I. Lelios, F. L. Heppner, J. Kipnis, D. Merkler, M. Greter, B. Becher, High-dimensional single-cell mapping of central nervous system immune cells reveals distinct myeloid subsets in health, aging, and disease. *Immunity* **48**, 380–395.e6 (2018).

65. N. Villacampa, M. T. Heneka, Microglia: You'll never walk alone! *Immunity* **48**, 195–197 (2018).

66. I. Bechmann, J. Priller, A. Kovac, M. Böntert, T. Wehner, F. F. Klett, J. Bohsung, M. Stuschke, U. Dirnagl, R. Nitsch, Immune surveillance of mouse brain perivascular spaces by blood-borne macrophages. *Eur. J. Neurosci.* **14**, 1651–1658 (2001).

67. H. Li, G.-X. Zhang, Y. Chen, H. Xu, D. C. Fitzgerald, Z. Zhao, A. Rostami, CD11c $^{+}$ CD11b $^{+}$ dendritic cells play an important role in intravenous tolerance and the suppression of experimental autoimmune encephalomyelitis. *J. Immunol.* **181**, 2483–2493 (2008).

68. R. Yamasaki, H. Lu, O. Butovsky, N. Ohno, A. M. Rietsch, R. Cialic, P. M. Wu, C. E. Doykan, J. Lin, A. C. Cotleur, G. Kidd, M. M. Zorlu, N. Sun, W. Hu, L. Liu, J.-C. Lee, S. E. Taylor, L. Uehlein, D. Dixon, J. Gu, C. M. Floruta, M. Zhu, I. F. Charo, H. L. Weiner, R. M. Ransohoff, Differential roles of microglia and monocytes in the inflamed central nervous system. *J. Exp. Med.* **211**, 1533–1549 (2014).

69. M. Inoue, K. L. Williams, M. D. Gunn, M. L. Shinohara, NLRP3 inflammasome induces chemotactic immune cell migration to the CNS in experimental autoimmune encephalomyelitis. *Proc. Natl. Acad. Sci. U.S.A.* **109**, 10480–10485 (2012).

70. A. Lutterotti, S. Yousef, A. Sputtek, K. H. Stürner, J.-P. Stellmann, P. Breiden, S. Reinhardt, C. Schulze, M. Bester, C. Heesen, S. Schippling, S. D. Miller, M. Sospedra, R. Martin, Antigen-specific tolerance by autologous myelin peptide-coupled cells: A phase 1 trial in multiple sclerosis. *Sci. Transl. Med.* **5**, 188ra75 (2013).

71. H. I. McFarland, A. A. Lobito, M. M. Johnson, J. T. Nyswaner, J. A. Frank, G. R. Palardy, N. Tresser, C. P. Genain, J. P. Mueller, L. A. Matis, M. J. Lenardo, Determinant spreading associated with demyelination in a nonhuman primate model of multiple sclerosis. *J. Immunol.* **162**, 2384–2390 (1999).

72. C. L. Vanderlugt, S. D. Miller, Epitope spreading in immune-mediated diseases: Implications for immunotherapy. *Nat. Rev. Immunol.* **2**, 85–95 (2002).

73. J. Li, D. Qiu, Y. Liu, J. Xiong, Y. Wang, X. Yang, X. Fu, L. Zheng, G. Luo, M. Xing, Y. Wu, Cytomembrane infused polymer accelerating delivery of myelin antigen peptide to treat experimental autoimmune encephalomyelitis. *ACS Nano* **12**, 11579–11590 (2018).

74. Z. Hunter, D. P. McCarthy, W. T. Yap, C. T. Harp, D. R. Getts, L. D. Shea, S. D. Miller, A biodegradable nanoparticle platform for the induction of antigen-specific immune tolerance for treatment of autoimmune disease. *ACS Nano* **8**, 2148–2160 (2014).

75. G. Contarini, P. Giusti, S. D. Skaper, Active induction of experimental autoimmune encephalomyelitis in C57BL/6 Mice. *Methods Mol. Biol.* **1727**, 353–360 (2018).

76. M. J. Farrar, I. M. Bernstein, D. H. Schlafer, T. A. Cleland, J. R. Fetcho, C. B. Schaffer, Chronic in vivo imaging in the mouse spinal cord using an implanted chamber. *Nat. Methods* **9**, 297–302 (2012).

77. B. Schattling, K. Steinbach, E. Thies, M. Kruse, A. Menigoz, F. Ufer, V. Flockerzi, W. Brück, O. Pongs, R. Vennekens, M. Kneussel, M. Freichel, D. Merkler, M. A. Friese, TRPM4 cation channel mediates axonal and neuronal degeneration in experimental autoimmune encephalomyelitis and multiple sclerosis. *Nat. Med.* **18**, 1805–1811 (2012).

78. C. L. Lucas, H. S. Kuehn, F. Zhao, J. E. Niemela, E. K. Deenick, U. Palendira, D. T. Avery, L. Moens, J. L. Cannons, M. Biancalana, J. Stoddard, W. Ouyang, D. M. Frucht, V. K. Rao, T. P. Atkinson, A. Agharahimi, A. A. Hussey, L. R. Folio, K. N. Olivier, T. A. Fleisher, S. Pittaluga, S. M. Holland, J. I. Cohen, J. B. Oliveira, S. G. Tangye, P. L. Schwartzberg, M. J. Lenardo, G. Uzel, Dominant-activating germline mutations in the gene encoding the PI(3)K catalytic subunit p110δ result in T cell senescence and human immunodeficiency. *Nat. Immunol.* **15**, 88–97 (2014).

79. S. Hugues, A. Scholer, A. Boissonnas, A. Nussbaum, C. Combadière, S. Amigorena, L. Fetler, Dynamic imaging of chemokine-dependent $CD8^+$ T cell help for $CD8^+$ T cell responses. *Nat. Immunol.* **8**, 921–930 (2007).

80. A. Boissonnas, L. Fetler, I. S. Zeelenberg, S. Hugues, S. Amigorena, In vivo imaging of cytotoxic T cell infiltration and elimination of a solid tumor. *J. Exp. Med.* **204**, 345–356 (2007).

81. A. J. Wilk, A. Rustagi, N. Q. Zhao, J. Roque, G. J. Martinez-Colon, J. L. McKechnie, G. T. Ivison, T. Ranganath, R. Vergara, T. Hollis, L. J. Simpson, P. Grant, A. Subramanian, A. J. Rogers, C. A. Blish, A single-cell atlas of the peripheral immune response in patients with severe COVID-19. *Nat. Med.* **26**, 1070–1076 (2020).